

COMBINATORIAL EQUIVALENCE OF REAL MODULI SPACES

SATYAN L. DEVADOSS

INTRODUCTION

The Riemann moduli space \mathcal{M}_g^n of surfaces of genus g with n marked points has become a central object in mathematical physics. Its importance was emphasized by Grothendieck in his famous *Esquisse d'un programme*. The special case \mathcal{M}_0^n is a building block leading to higher genera, playing a crucial role in the theory of Gromov-Witten invariants, symplectic geometry, and quantum cohomology. There is a Deligne-Knudsen-Mumford compactification $\overline{\mathcal{M}}_0^n$ of this space coming from Geometric Invariant Theory which allows collisions of points of the configuration space. This description comes from the repulsive potential observed by quantum physics: Pushing particles together creates a spherical bubble onto which the particles escape [11]. In other words, as points try to collide, the result is a new bubble fused to the old at the point of collision where the collided points are now on the new bubble. The phenomena is dubbed as *bubbling*; the resulting structure is called a *bubble-tree*.

Our work is motivated by the *real* points $\overline{\mathcal{M}}_0^n(\mathbb{R})$ of this space, the set of points fixed under complex conjugation. These real moduli spaces have importance in their own right, beginning to appear in many areas. For instance, Goncharov and Manin [7] recently introduce $\overline{\mathcal{M}}_0^n(\mathbb{R})$ in discussing ζ -motives and the geometry of $\overline{\mathcal{M}}_0^n$.

The real spaces, unlike their complex counterparts, have a tiling that is inherently present in them. This allows one to understand and visualize them using tools ranging from arrangements, to reflection groups, to combinatorics. This article began in order to understand why the two pictures in Figure 13 are the same: Both of them have identical cellulation, tiled by 60 polyhedra known as associahedra. It was Kapranov who first noticed this relationship, relating $\overline{\mathcal{M}}_0^n(\mathbb{R})$ to the braid arrangement of hyperplanes. We provide an intuitive, combinatorial formulation of $\overline{\mathcal{M}}_0^n(\mathbb{R})$ in order to show the equivalence in the figure. Along the way, we provide a construction of the associahedron from truncations of certain products of simplices.

A configuration space of n ordered, distinct particles on a manifold M is defined as

$$C_n(M) = M^n - \Delta, \quad \text{where } \Delta = \{(x_1, \dots, x_n) \in M^n \mid \exists i, j, x_i = x_j\}.$$

1991 *Mathematics Subject Classification*. Primary 14P25, Secondary 90C48, 52B11.
The author was partially supported by NSF grant DMS-0310354.

The recent work in physics around conformal field theories has led to an increased interest in the configuration space of n labeled points on the projective line. The focus is on a quotient of this space by $\mathbb{P}\mathrm{GL}_2(\mathbb{C})$, the affine automorphisms on $\mathbb{C}\mathbb{P}^1$. The resulting variety \mathcal{M}_0^n is the moduli space of Riemann spheres with n labeled punctures.

Definition 1. The *real* moduli space of n -punctured Riemann spheres is

$$\mathcal{M}_0^n(\mathbb{R}) = C_n(\mathbb{R}\mathbb{P}^1)/\mathbb{P}\mathrm{GL}_2(\mathbb{R}),$$

where $\mathbb{P}\mathrm{GL}_2(\mathbb{R})$ sends three of the points to $0, 1, \infty$.

This moduli space encapsulates the new constructions of the associahedra developed below.

THE SIMPLEX

For a given manifold M , the symmetric group \mathbb{S}_n acts freely on the configuration space $C_n(M)$ by permuting the coordinates, and the quotient manifold $B_n(M) = C_n(M)/\mathbb{S}_n$ is the space of n unordered, distinct particles on M . The closure of this space in the product is denoted by $B_n\langle M \rangle$. Let $\mathrm{Aff}(\mathbb{R})$ be the group of affine transformations of \mathbb{R} generated by translating and scaling. The space $B_{n+2}(\mathbb{R})/\mathrm{Aff}(\mathbb{R})$ is the open n -simplex: The leftmost of the $n+2$ particles in \mathbb{R} is translated to 0 and the rightmost is dilated to 1, and we have the subset of \mathbb{R}^n where

$$(1) \quad 0 < x_1 < x_2 < \cdots < x_{n-1} < x_n < 1.$$

The closure of this space is the n -simplex Δ_n whose codimension k face can be identified by the set of points with exactly k equalities of (1).

Notation. If we let I_2 denote the unit interval $[0, 1] \subset \mathbb{R}$ with *fixed* particles at the two endpoints, then the n -simplex can be viewed as the closure $B_n\langle I_2 \rangle$. We use bracket notation to display this visually: Denote the n particles on the interval I_2 as nodes on a path, with the fixed ones as nodes shaded black. When the inequalities of (1) become equalities, draw brackets around the nodes representing the set of equal points on the interval. For example, $\bullet\text{---}\circ\text{---}\circ\text{---}\circ\text{---}\circ\text{---}\circ\text{---}\bullet$ corresponds to the configuration

$$0 < x_1 < x_2 = x_3 = x_4 < x_5 < x_6 = 1.$$

We call such a diagram a *bracketing*. Figure 1 depicts Δ_2 and Δ_3 along with a labeling of vertices and edges.

The associahedron is a convex polytope originally defined by Stasheff [12] for use in homotopy theory in connection with associativity properties of H -spaces. It continues to appear in a vast number of mathematical fields, currently leading to numerous generalizations.

Definition 2. Let $\mathfrak{A}(n)$ be the poset of bracketings of a path with n nodes, ordered such that $a \prec a'$ if a is obtained from a' by adding new brackets. The *associahedron* K_n is a convex polytope of dimension $n-2$ whose face poset is isomorphic to $\mathfrak{A}(n)$.

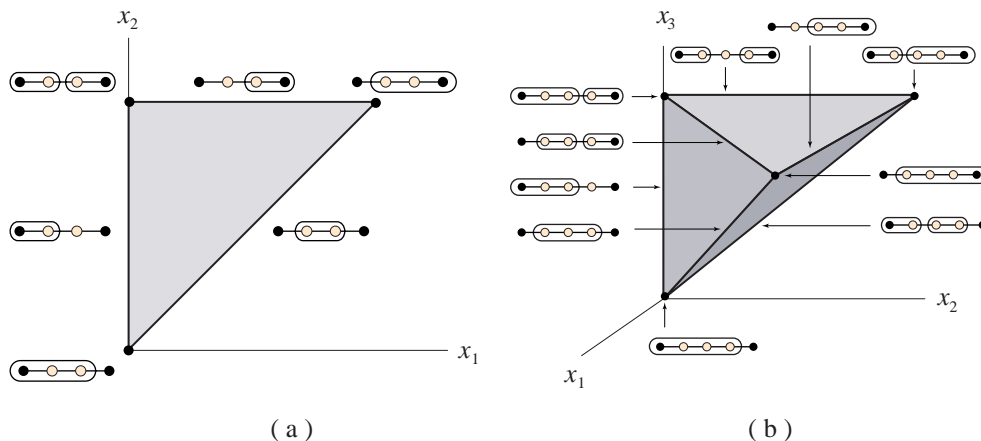


FIGURE 1. Labeling of vertices and edges of Δ_2 and Δ_3 .

Example 3. Figure 2 shows the two-dimensional K_4 as the pentagon. Each edge of K_4 has one set of brackets, whereas each vertex has two. Figure 4(b) depicts K_5 with only the *facets* (codimension one faces) labeled here.

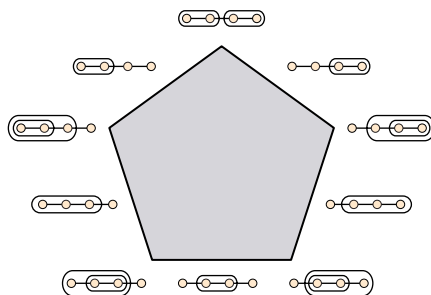


FIGURE 2. Associahedron K_4 .

Two bracketings are *compatible* if the brackets of the superimposition do not intersect. Figure 3 shows an example of two compatible bracketings (a) and (b). It follows from the definition of K_n that two faces are adjacent if and only if their bracketings are compatible. Furthermore, the face of intersection is labeled by the superimposed image (c).

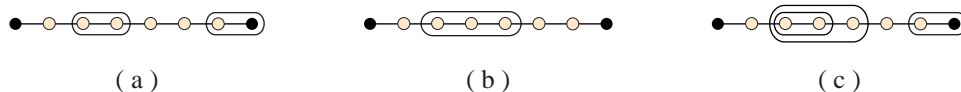


FIGURE 3. Compatibility of bracketings.

A well-known construction of the associahedron from the simplex via truncating hyperplanes is given in the Appendix of [13]. A reformulation from the perspective of configuration spaces is as follows:

Remark. An n -polytope is *simple* if every k -face is contained in $n - k$ facets. The simplex is a simple polytope and a truncation of a simple polytope remains simple.

Construction 1. Choose the collection \mathcal{C} of codimension k faces of the n -simplex $B_n\langle I_2 \rangle$ which correspond to configurations where $k + 1$ adjacent particles collide. Truncating elements of \mathcal{C} in increasing order of dimension results in K_{n+2} .

Proof. We show the construction to be well defined, that truncation is a commutative operation for faces of the same dimension. In other words, if two codimension k faces F_1 and F_2 of \mathcal{C} intersect at a codimension $(k + 1)$ face G , then G is in \mathcal{C} . Indeed, this is an immediate consequence of what it means to be an element of \mathcal{C} : Since F_1 and F_2 each have k adjacent equalities in (1), then G must have $k + 1$ adjacent equalities since $G = F_1 \cap F_2$.

We show that the face poset of Δ_n , as faces in \mathcal{C} are truncated, changes to the face poset of K_{n+2} . Let F be a codimension k face in \mathcal{C} and \mathcal{K}_F be the collection of faces of the polytope that intersect F . By definition of truncation, there exists a bijection $\phi : Y_F \rightarrow \mathcal{K}_F$ between the faces of Y_K to elements in \mathcal{K}_F . Label each face f of Y_F with the superimposition of the bracket labelings of F and $\phi(f)$. It is clear the labelings of F and $\phi(f)$ will be compatible from the adjacency relation of the faces.

Since our polytope is simple, truncating F replaces it with a facet $Y_F = F \times \Delta_{k-1}$. Since F is defined by $k + 1$ adjacent particles colliding, the simplex Δ_{k-1} introduced in the truncation inherits the bracket labeling of $B_{k+1}\langle I_2 \rangle$. Indeed, we are not allowing the $k + 1$ particles to collide at once, but resolving all possible orderings in which the collisions could occur. After iterating this procedure over all elements of \mathcal{C} , the face poset of the resulting polytope will be isomorphic to K_{n+2} . \square

Remark. A proof of this construction using face posets and bracketings in a general context of graphs is given in [1, §5].

Example 4. Figure 4(a) shows K_4 after truncating the two vertices  and  of Δ_2 given in Figure 1. Each vertex is now replaced by a facet given the same labeling as the original vertices. However, the new vertices introduced by shaving are labeled with nested parentheses, seen as the superimposition of the respective diagrams. Similarly, Figure 4(b) displays K_5 with facets diagrams after first shaving two vertices and then three edges of Δ_3 . Compare this with Figure 1.

This construction of K_n from the simplex is the real *Fulton-MacPherson* [6] compactification of the configuration space $B_n(I_2)$. We denote this as $B_n[I_2]$. Casually speaking, one is not only interested in when k adjacent particles collide, but in resolving that singularity

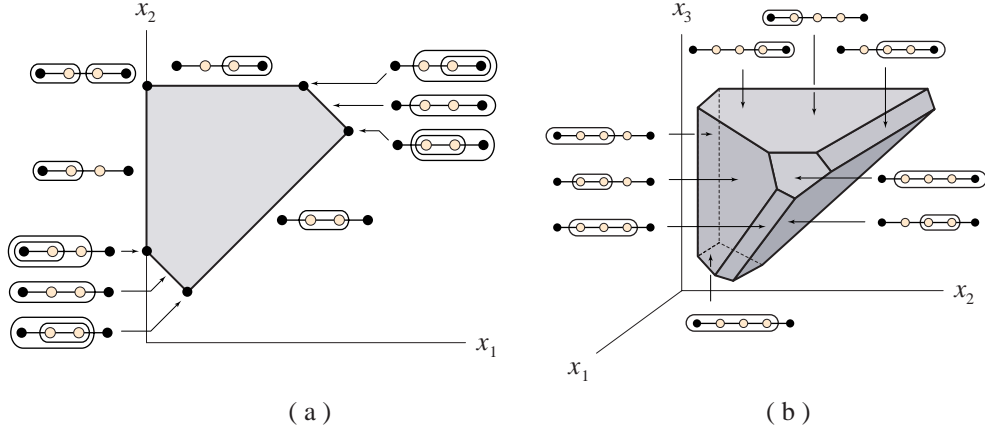


FIGURE 4. (a) Vertices and edges of K_4 labeled. (b) Facets of K_5 labeled.

by ordering the collisions. For example,  not just conveys that the three particles have collided, but that the first two particles collided before meeting with the third.

Remark. In the original closed simplex, the number of equalities (collisions) correspond to the codimension of the cell. After the compactification, the codimension is given by the number of brackets.

PRODUCTS OF SIMPLICES

We extend the notions above to triple products of simplices. In doing so, we see new combinatorial constructions of the associahedron. Let S_3 denote a circle with three distinct fixed particles. The space $B_n\langle S_3 \rangle$ is combinatorially equivalent to the product of three simplices $\Delta_i \times \Delta_j \times \Delta_k$, with $i + j + k = n$. Indeed, the different types of simplicial products depend on how the n particles are partitioned among the three regions, each region defined between two fixed particles. Note that each configuration of k particles which fall between two fixed particles give rise to the k -simplex $B_k\langle I_2 \rangle$.

Example 5. There are three possibilities when $n = 3$: The simplex Δ_3 , the prism $\Delta_2 \times \Delta_1$, and the cube $\Delta_1 \times \Delta_1 \times \Delta_1$ as presented in Figure 5.

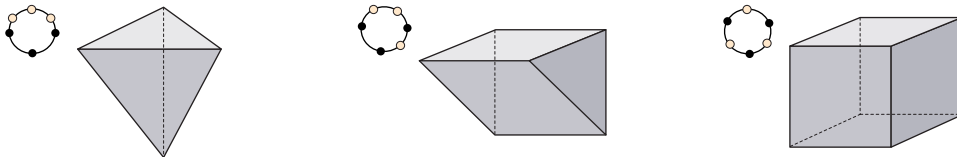


FIGURE 5. Three types of simplicial products with three particles.

Construction 2. Let $\mathfrak{B}(n)$ be the poset of bracketings of S_3 with $n - 2$ additional nodes partitioned into the three regions, where no bracket contains more than one of the three marked nodes of S_3 . Order them such that $b < b'$ if b is obtained from b' by adding new brackets. The face poset $\mathfrak{A}(n)$ of K_n is isomorphic to $\mathfrak{B}(n)$.

Choose any one of the three fixed particles of S_3 , call it p . The particles of $S_3 - p$ can be viewed as n particles on the line. If a bracket does not contain p , preserve this bracketing on the line; see Figure 6(a). If a bracket does contain p , choose the bracket on the line that encloses the complementary set of particles; see Figure 6(b). This is a bijection of posets since a bracket on S_3 can contain at most one fixed particle.

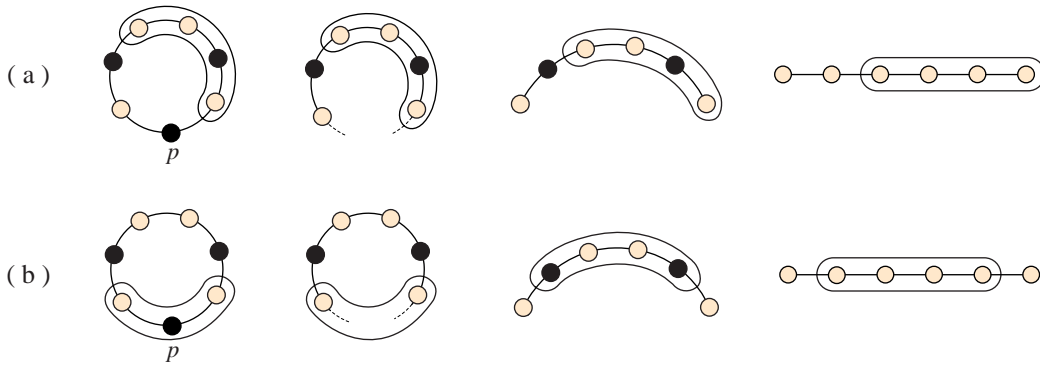


FIGURE 6. Bijection from $\mathfrak{B}(n)$ to $\mathfrak{A}(n)$.

Remark. Each partition of the $n - 2$ nodes in S_3 gives rise to a different poset that is isomorphic to $\mathfrak{A}(n)$.

We look at the compactification $B_n[S_3]$. Analogous to Construction 1, we specify certain faces of $\Delta_x \times \Delta_y \times \Delta_z$ to be truncated, namely the codimension k faces where $k + 1$ adjacent particles collide. Indeed, each facet of the polytope $B_n[S_3]$ will correspond to a unique way of adding a bracket around the $n + 3$ particles (n free and 3 fixed) in S_3 . The restriction will be that no bracket will include more than one fixed particle, for this would imply that the fixed particles inside the bracket would be identified.

Example 6. Figure 7(a) shows the prism in Figure 5 with labeling of the top dimensional faces. Figure 7(b) shows the labeling of the vertices, along with the new facet obtained by shaving a vertex (codimension three) where four adjacent particles collide. Similarly, part (c) is the labeling of the edges, along with the truncation of three of them. Notice that the resulting polytope is combinatorially equivalent to K_5 .

Construction 3. Choose the collection of codimension k faces of $\Delta_x \times \Delta_y \times \Delta_z$ which correspond to configurations where $k + 1$ adjacent particles collide. Truncating elements of this collection in increasing order of dimension results in $K_{x+y+z+2}$.

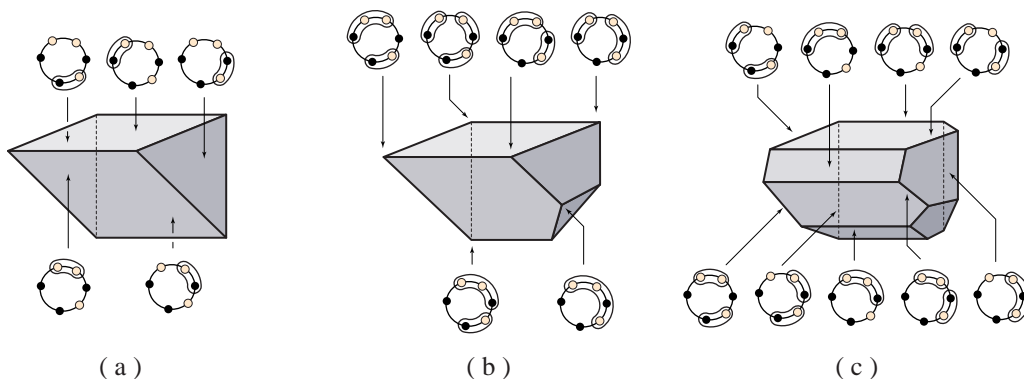


FIGURE 7. Truncation and labeling of $\Delta_2 \times \Delta_1$.

Since $\Delta_x \times \Delta_y \times \Delta_z$ is simple, truncating a codimension k face F replaces it with a product $F \times \Delta_{k-1}$. Label the faces of $F \times \Delta_{k-1}$ with superimposition of neighboring faces. Truncating all elements produces a face poset structure isomorphic to $\mathfrak{B}(n)$. Then use Construction 2.

Corollary 7. *Let $p_k(n)$ be partitions of n into exactly k parts. There are*

$$p_3(n - 3) + p_2(n - 2) + 1$$

different ways of obtaining K_n from iterated truncations of simplicial products.

Indeed, for each triple product of simplices, there exists a method to obtain the associahedron from iterated truncations of faces. Figure 8 shows K_5 from truncations of the three polytopes in Figure 5. Figure 12 displays the *Schlegel diagrams* of four 4-polytopes, the (a) 4-simplex, (b) tetrahedral prism, (c) product of triangles, and (d) product of triangle and square. Each is truncated to (combinatorial equivalent) K_6 associahedra, each with seven K_5 and seven pentagonal prism facets.

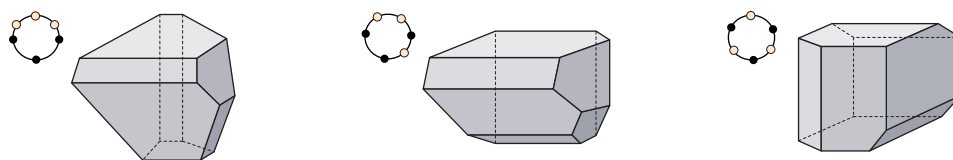


FIGURE 8. Iterated truncations of polytopes resulting in K_5 .

THE BRAID ARRANGEMENT

We relate the combinatorial structure of the associahedron to a tiling of spaces. This yields an elegant framework for associating Coxeter complexes to certain moduli spaces. We begin with some background [2]. The symmetric group \mathfrak{S}_{n+2} is a finite reflection group acting on

\mathbb{R}^{n+2} as reflections (ij) across the hyperplanes $\{x_i = x_j\}$, forming the *braid arrangement* of hyperplanes \mathcal{H} . The *essential* subspace under the action of \mathbb{S}_{n+2} is the hyperplane V^{n+1} defined by $\sum x_i = 0$. This space is tiled by simplicial cones, defined by $n + 1$ inequalities

$$(2) \quad x_{i_1} \leq x_{i_2} \leq \cdots \leq x_{i_{n+1}} \leq x_{i_{n+2}}.$$

Let $\mathbb{S}V^n$ be the sphere in V^{n+1} . The braid arrangement gives these spaces a cellular decomposition into $(n + 2)!$ chambers. Each chamber of $\mathbb{S}V^n$ is an n -simplex, defined by (2) where not all inequalities are equalities.¹

Definition 8. A *cellulation* of a manifold M is formed by gluing together polytopes using combinatorial equivalence of their faces, together with the decomposition of M into its cells.

Proposition 9. Let $C_n\langle\mathbb{R}\rangle$ denote the closure of $C_n(\mathbb{R})/\text{Aff}(\mathbb{R})$. Then $C_n\langle\mathbb{R}\rangle$ has the same cellulation as $\mathbb{S}V^{n-2}$.

Proof. Let $\vec{a}_1, \dots, \vec{a}_n \in \mathbb{R}^n$ such that $\vec{a}_i = -(\vec{e}_1 + \cdots + \vec{e}_n) + n\vec{e}_i$. Note that $\sum \vec{a}_i = 0$, $\vec{a}_i \in \langle 1, \dots, 1 \rangle^\perp$, and

$$\vec{a}_i \cdot \vec{a}_j = \begin{cases} n^2 - n & \text{for } i = j \\ -n & \text{for } i \neq j. \end{cases}$$

Let $v = \langle v_1, \dots, v_n \rangle \in C_n\langle\mathbb{R}\rangle$. Define the map $\varphi : C_{n+2}\langle\mathbb{R}\rangle \rightarrow \mathbb{S}V^{n-2}$ such that

$$\varphi(v) = \frac{\sum v_i \vec{a}_i}{|\sum v_i \vec{a}_i|}.$$

An ordering of the n points $v_1 \leq \cdots \leq v_n$ defines a chamber in $C_n\langle\mathbb{R}\rangle$. Similarly, a chamber of $\mathbb{S}V^{n-2}$ corresponds to an ordering of elements as in equation (2). We show that $\varphi(v_1) \leq \cdots \leq \varphi(v_n)$. For each $v_i \leq v_j$,

$$\vec{a}_j \cdot \varphi(v) - \vec{a}_i \cdot \varphi(v) = n^2(v_i - v_j) \geq 0.$$

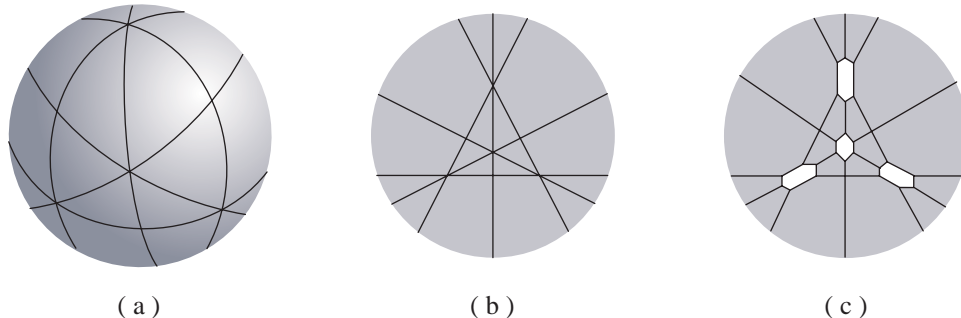
Now $\sum \varphi(v_i) = 0$ since $\varphi(v_i) \in \mathbb{S}V^{n-2}$, so

$$\vec{a}_i \cdot \varphi(v) = -(\varphi(v_1) + \cdots + \varphi(v_n)) + n\varphi(v_i) = n\varphi(v)_i,$$

and thus $\varphi(v_i) \leq \varphi(v_j)$ preserving the chamber structure. It is easy to show that φ is a homeomorphism. Since a codimension k face of both spaces is where exactly k equalities in $\langle v_1, \dots, v_n \rangle$ occur, the cellulation naturally follows. \square

Indeed, each simplicial chamber of $\mathbb{S}V^n$ corresponds to an arrangement of $n + 2$ particles on an interval, resulting in $B_n\langle I_2 \rangle$. A chamber of $\mathbb{P}V^n$, the projective sphere in V^{n+1} , identifies two antipodal chambers of $\mathbb{S}V^n$. Figures 9(a) and 9(b) depict the $n = 2$ case. Observe that quotienting by translations of $\text{Aff}(\mathbb{R})$ removes the inessential component of the arrangement, scaling (by a factor of $s \in \mathbb{R}^+$) pertains to intersecting V^n with the sphere, and *dilating* (by a factor of $s \in \mathbb{R}^*$) results is $\mathbb{P}V^n$.

¹The point where all equalities exist is at the cone point, which is not contained in the sphere.


 FIGURE 9. (a) \mathbb{S}^2 , (b) $\mathbb{P}V^2$ and (c) $\mathbb{P}V^2_{\#}$.

The collection of hyperplanes $\{x_i = 0 \mid i = 1, \dots, n\}$ of \mathbb{R}^n generates the *coordinate arrangement*. Let M be a manifold and $D \subset M$ a union of codimension one submanifolds which dissects M into convex polytopes. A crossing (of D) in M is *normal* if it is locally isomorphic to a coordinate arrangement. If every crossing is normal, then M is *right angled*. An operation which transforms any crossing into a normal crossing involves the algebro-geometric concept of a blow-up.

Definition 10. For a linear subspace X of a vector space Y , we *blow up* $\mathbb{P}Y$ along $\mathbb{P}X$ by removing $\mathbb{P}X$, replacing it with the sphere bundle associated to the normal bundle of $\mathbb{P}X \subset \mathbb{P}Y$, and then projectifying the bundle.

Blowing up a subspace of a cell complex truncates faces of polytopes adjacent to the subspace. As mentioned above with truncations, a general collection of blow-ups is usually non-commutative in nature; in other words, the order in which spaces are blown up is important. For a given arrangement, De Concini and Procesi [4] establish the existence (and uniqueness) of a *minimal building set*, a collection of subspaces for which blow-ups commute for a given dimension, and for which the resulting space is right angled.

For an arrangement of hyperplanes, the method developed by De Concini and Procesi compactifies their complements by iterated blow-ups of the minimal building set. In the case of the arrangement $X^n - C_n(X)$, their procedure yields the Fulton-MacPherson compactification of $C_n(X)$. We can view $\mathbb{P}V^n$ as a configuration space, where the codimension k elements of the minimal building set are the subspaces

$$(3) \quad x_{i_1} = x_{i_2} = \dots = x_{i_{k+1}}$$

of $\mathbb{P}V^n$ where $k+1$ adjacent particles collide. Let $\mathbb{P}V^n_{\#}$ denote the space $\mathbb{P}V^n$ after iterated blow-ups along elements of the minimal building set in increasing order of dimension.

Theorem 11. [8] $\mathbb{P}V^n_{\#}$ is tiled by $\frac{1}{2}(n+2)!$ copies of associahedra K_{n+2} .

Indeed, this is natural since the blow-up of all codimension k subspaces (3) truncates the collection \mathcal{C} of codimension k faces of the simplex defined in Construction 1. Figure 9(c) shows $\mathbb{P}V_{\#}^2$ tiled by 12 associahedra K_4 .

A combinatorial construction of $\mathbb{P}V_{\#}^n$ is presented in [5] by gluing faces of the $\frac{1}{2}(n+2)!$ copies of associahedra. Associate to each K_{n+2} a path with $n+2$ labeled nodes, with two such labelings equivalent up to reflection. Thus each face of an associahedron is identified with a labeled bracketing. A *twist* along a bracket reflects all the elements within the bracket (both labeled nodes and brackets).

Theorem 12. [5] *Two bracketings of a path with $n+2$ labeled nodes, corresponding to faces of K_{n+2} , are identified in $\mathbb{P}V_{\#}^n$ if there exists a sequence of twists along brackets from one diagram to another.*

Each element of the minimal building set corresponds to subspaces such as (3), where blowing up the subspace seeks to resolve the *order* in which collisions occur at such intersections. Crossing from a chamber through the blown-up cell into its antipodal one in the arrangement (from projectifying the bundle) corresponds to reflecting the elements $\{x_{i_1}, x_{i_2}, \dots, x_{i_{k+1}}\}$ in the ordering. Blowing up a minimal cell identifies faces across the antipodal chambers, with twisting along diagonals mimicking gluing antipodal faces after blow-ups.

Figure 10 shows a local tiling of $\mathbb{P}V_{\#}^2$ by K_4 , with edges (in pairs) and vertices (in fours) being identified after twists. Notice that after twisting a bracket containing a fixed node, the new right- (or left-)most node becomes fixed by the action of $\text{Aff}(\mathbb{R})$.

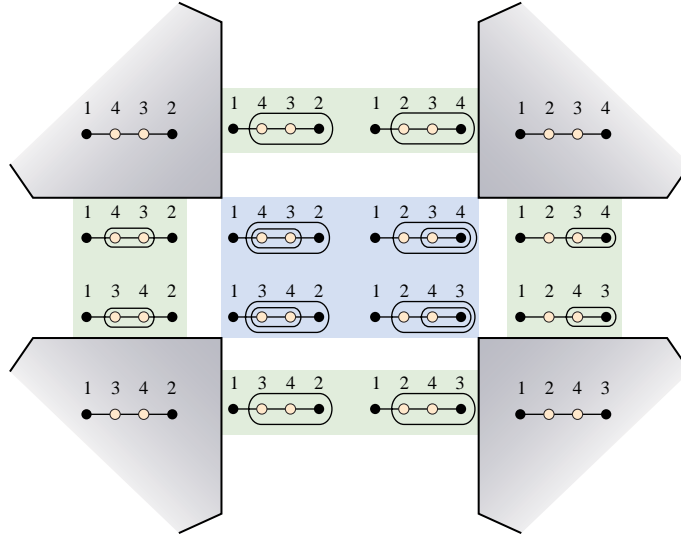


FIGURE 10. A local tiling of $\mathbb{P}V_{\#}^2$ displaying twisting.

Remark. This immediately shows $\mathbb{P}V_{\#}^n$ to be right angled: A codimension k face of an associahedron of $\mathbb{P}V_{\#}^n$ has k brackets, with each twist along a bracket moving to an adjacent chamber. There are 2^k such possible combinations of twists, giving a normal crossing at each face.

KAPRANOV'S THEOREM

We start with properties of the manifold before compactification.

Proposition 13. *Let $\mathbb{P}V_{\mathcal{H}}^n$ denote $\mathbb{P}V^n$ minus the braid arrangement \mathcal{H} . Then $\mathcal{M}_0^{n+3}(\mathbb{R})$ is isomorphic to $\mathbb{P}V_{\mathcal{H}}^n$.*

Proof. Let $(x_1, \dots, x_{n+3}) \in C_{n+3}(\mathbb{R}\mathbb{P}^1)$. Since a projective automorphism of \mathbb{P}^1 is uniquely determined by the images of three points, we can take $x_{n+1}, x_{n+2}, x_{n+3}$ to $0, 1, \infty$, respectively. Therefore,

$$\begin{aligned} \mathcal{M}_0^{n+3}(\mathbb{R}) &= \{(x_1, \dots, x_n) \in (\mathbb{R}\mathbb{P}^1)^n \mid x_i \neq x_j, x_i \neq 0, 1, \infty\} \\ &= \{(x_1, \dots, x_n) \in (\mathbb{R}^1)^n \mid x_i \neq x_j, x_i \neq 0, 1\} \\ &= \{(x_1, \dots, x_n) \in \mathbb{R}^n \mid x_i \neq x_j, x_i \neq 0, 1\}. \end{aligned}$$

We construct a space isomorphic to $\mathbb{P}V_{\mathcal{H}}^n$: Intersect $C_{n+2}(\mathbb{R})$ with the hyperplane $\{x_{n+2} = 0\}$ instead of the more symmetric hyperplane $\{\sum x_i = 0\}$ to obtain

$$\{(x_1, \dots, x_{n+1}) \in \mathbb{R}^{n+1} \mid x_i \neq x_j, x_i \neq 0\}.$$

We projectify by choosing the last coordinate to be one, resulting in

$$\{(x_1, \dots, x_n) \in \mathbb{R}^n \mid x_i \neq x_j, x_i \neq 0, 1\}.$$

This is isomorphic to $\mathbb{P}V_{\mathcal{H}}^n$, and the equivalence is shown. \square

Since $\mathcal{M}_0^{n+3}(\mathbb{R})$ is isomorphic to the n -torus $(\mathbb{R}\mathbb{P}^1)^n$ minus the hyperplanes $\{x_i = x_j, x_i = 0, 1, \infty\}$, it follows that

$$\mathcal{M}_0^{n+3}(\mathbb{R}) = C_n(S_3)$$

with the three fixed points identified to $0, 1, \infty$. As $\mathbb{P}V^n$ is tiled by simplices, the closure of $\mathcal{M}_0^{n+3}(\mathbb{R})$ is tiled by triple product of simplices, namely $B_n\langle S_3 \rangle$. The compactification $\overline{\mathcal{M}}_0^{n+3}(\mathbb{R})$ is obtained by iterated blow-ups of $\mathcal{M}_0^{n+3}(\mathbb{R})$ along non-normal crossings in increasing order of dimension [13, §3]. The codimension k subspaces

$$x_{i_1} = x_{i_2} = \dots = x_{i_{k+1}}$$

and

$$x_{i_1} = x_{i_2} = \dots = x_{i_k} = f,$$

where $f \in \{0, 1, \infty\}$, form the minimal building set, configurations where $k + 1$ adjacent particles collide on S_3 . Similar to $\mathbb{P}V_{\#}^n$, the blow-up of all minimal subspaces truncate the chambers into associahedra as defined by Construction 3.

Although the closures of $\mathcal{M}_0^{n+3}(\mathbb{R})$ and $\mathbb{P}V_{\mathcal{H}}^n$ are clearly different (the torus T^n and $\mathbb{R}\mathbb{P}^n$ respectively), Kapranov [8, §4] remarkably noticed that their compactifications are homeomorphic.² We give an alternate proof of his theorem.

Theorem 14. $\overline{\mathcal{M}_0^{n+3}(\mathbb{R})}$ is homeomorphic to $\mathbb{P}V_{\#}^n$. Moreover, they have identical cellulation.

Proof. Both $\overline{\mathcal{M}_0^{n+3}(\mathbb{R})}$ and $\mathbb{P}V_{\#}^n$ have the same number of chambers by Proposition 13. Each tile of the closure of $\mathcal{M}_0^{n+3}(\mathbb{R})$ corresponds to a triple product of simplices. Since the building set of $\mathcal{M}_0^{n+3}(\mathbb{R})$ corresponds to the faces of $B_n\langle S_3 \rangle$ to be truncated in Construction 3, $\overline{\mathcal{M}_0^{n+3}(\mathbb{R})}$ is tiled by associahedra K_{n+2} , more precisely by $B_n[S_3]$. We still need to show this tiling is identical to that of $\mathbb{P}V_{\#}^n$.

As in Theorem 12, crossing a chamber through the blown-up cell into its antipodal one in the arrangement corresponds to reflecting the elements within a bracket of $B_n[S_3]$. This is encapsulated by the twisting operation on S_3 , similar to $\mathbb{P}V_{\#}^n$. Finally, Construction 2 gives us the isomorphism of cellulations between $\overline{\mathcal{M}_0^{n+3}(\mathbb{R})}$ and $\mathbb{P}V_{\#}^n$. \square

Example 15. The top diagrams of Figure 11 present (a) $\mathbb{P}V_{\mathcal{H}}^2$ tiled by open simplices, and (b) $\mathcal{M}_0^5(\mathbb{R})$, the 2-torus minus the hyperplanes $\{x_1 = x_2, x_i = 0, 1, \infty\}$ tiled by open simplices and squares. After minimal blow-ups, the resulting (homeomorphic) manifolds are (a) $\#^5 \mathbb{R}\mathbb{P}^2$ and (b) $T^2 \#^3 \mathbb{R}\mathbb{P}^2$, both tiled by 12 associahedra K_4 .

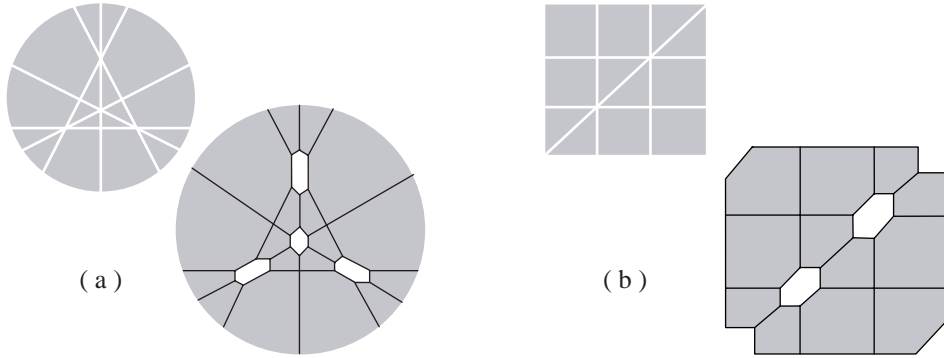


FIGURE 11. (a) $\mathbb{P}V_{\mathcal{H}}^2$ and (b) $\mathcal{M}_0^5(\mathbb{R})$ before and after compactification.

Example 16. Figure 13(a) shows $\mathbb{R}\mathbb{P}^3$ along with five vertices (shaded orange) and ten lines (shaded blue) blown-up resulting in $\mathbb{P}V_{\#}^3$. All chambers have been truncated from the simplex to K_5 . Figure 13(b) is the blow-up of the 3-torus into $\overline{\mathcal{M}_0^6}(\mathbb{R})$ along three vertices (orange) and ten lines (blue). Notice the appearance of the associahedra as in

²Kapranov actually proves a stronger result for the complex analog of the statement using Chow quotients of Grassmanians [9].

Figure 8. The resulting manifolds are homeomorphic, tiled by 60 associahedra. The lower dimensional moduli spaces $\mathbb{P}V_{\#}^2$ and $\overline{\mathcal{M}}_0^5(\mathbb{R})$ can be seen in the figures due to a product structure that is inherent in these spaces.

Remark. The iterated blow-up of the minimal building set (that is, the Fulton-MacPherson compactification) is the key to this equivalence. Iterated blow-ups along the *maximal* building set (also known as the *polydiagonal* compactification of Ulyanov), the collection of *all* crossings not just the non-normal ones, yield different manifolds for $\mathbb{P}V_{\#}^n$ and $\mathcal{M}_0^{n+3}(\mathbb{R})$. For example, the blow-up of $\mathbb{P}V_{\#}^2$ is homeomorphic to $\#^8 \mathbb{R}\mathbb{P}^2$ tiled by 12 hexagons (permutohedra) whereas $\mathcal{M}_0^5(\mathbb{R})$ is homeomorphic to $T^2 \#^9 \mathbb{R}\mathbb{P}^2$ tiled by 6 hexagons and 6 octagons.

CONCLUSION

Although the motivating ideas of $\overline{\mathcal{M}}_0^n$ are now classical, the real analog is starting to develop richly. We have shown $\overline{\mathcal{M}}_0^n(\mathbb{R})$ to be intrinsically related to the braid arrangement, the Coxeter arrangement of type A_n . By looking at other Coxeter groups, an entire array of compactified configuration spaces have recently been studied, generalizing $\overline{\mathcal{M}}_0^n(\mathbb{R})$ from another perspective [1]. Davis et al. [3, §5] have shown these novel moduli spaces to be aspherical, where all the homotopy properties are completely encapsulated in their fundamental groups. Furthermore, both $\overline{\mathcal{M}}_0^n(\mathbb{R})$ and $\mathbb{P}V_{\#}^n$ have underlying operad structures: The properties of $\overline{\mathcal{M}}_0^n(\mathbb{R})$ are compatible with the operad of planar rooted trees [10], whereas the underlying structure for $\mathbb{P}V_{\#}^n$ is the mosaic operad of hyperbolic polygons [5].

This area is highly motivated by other fields, such as string theory, combinatorics of polytopes, representation theory, and others. We think that $\overline{\mathcal{M}}_0^n(\mathbb{R})$ will play a deeper role with future developments in mathematical physics. In his *Esquisse*, Grothendieck referred to $\overline{\mathcal{M}}_0^5$ as ‘un petit joyau’. By looking at the real version of these spaces, we see structure determined by combinatorial tilings, jewels in their own right.

Acknowledgments. We thank Jim Stasheff for continued encouragement and Mike Carr, Ruth Charney, and Mike Davis for helpful discussions.

REFERENCES

1. S. Armstrong, M. Carr, S. Devadoss, E. Engler, A. Leininger, and M. Manapat, Coxeter complexes and graph-associahedra, preprint 2004.
2. K. S. Brown, *Buildings*, Springer-Verlag, New York, 1989.
3. M. Davis, T. Januszkiewicz, R. Scott, Nonpositive curvature of blowups, *Selecta Math.* **4** (1998), 491 - 547.
4. C. De Concini and C. Procesi, Wonderful models of subspace arrangements, *Selecta Math.* **1** (1995), 459-494.
5. S. Devadoss, Tessellations of moduli spaces and the mosaic operad, *Contemp. Math.* **239** (1999), 91-114.
6. W. Fulton, R. MacPherson, A compactification of configuration spaces, *Ann. Math.* **139** (1994), 183-225.
7. A. Goncharov, Y. Manin, Multiple ζ -motives and moduli spaces $\overline{\mathcal{M}}_{0,n}$, *Compos. Math.* **140** (2004), 1-14.
8. M. M. Kapranov, The permutoassociahedron, MacLane's coherence theorem, and asymptotic zones for the KZ equation, *J. Pure Appl. Alg.* **85** (1993), 119-142.
9. M. M. Kapranov, Chow quotients of grassmannians I, *Adv. in Sov. Math.* **16** (1993), 29-110.
10. T. Kimura, A. A. Voronov, J. Stasheff, On operad structures on moduli spaces and string theory, *Comm. Math. Phys.* **171** (1995), 1-25.
11. T. Parker, J. Wolfson, Pseudo-holomorphic maps and bubble trees, *J. Geom. Anal.* **3** (1993), 63-98.
12. J. Stasheff, Homotopy associativity of H -spaces, *Trans. Amer. Math. Soc.* **108** (1963), 275-292.
13. J. Stasheff (Appendix B coauthored with S. Shnider), From operads to "physically" inspired theories, *Contemp. Math.* **202** (1997), 53-81.

DEPARTMENT OF MATHEMATICS AND STATISTICS, WILLIAMS COLLEGE, WILLIAMSTOWN, MA 01267
E-mail address: satyan.devadoss@williams.edu

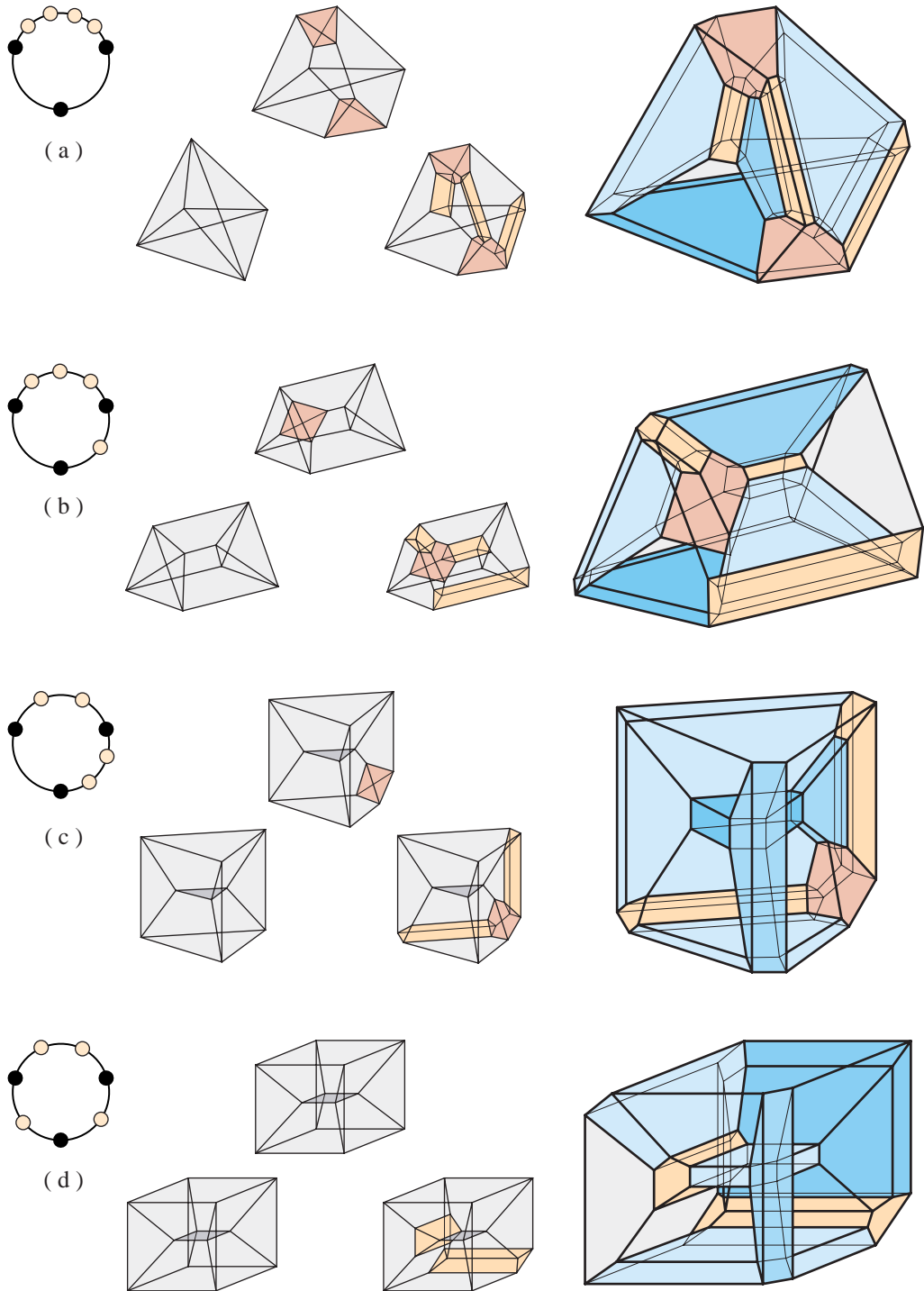


FIGURE 12. Schlegel diagrams of the iterated truncations of 4-polytopes resulting in K_6 .

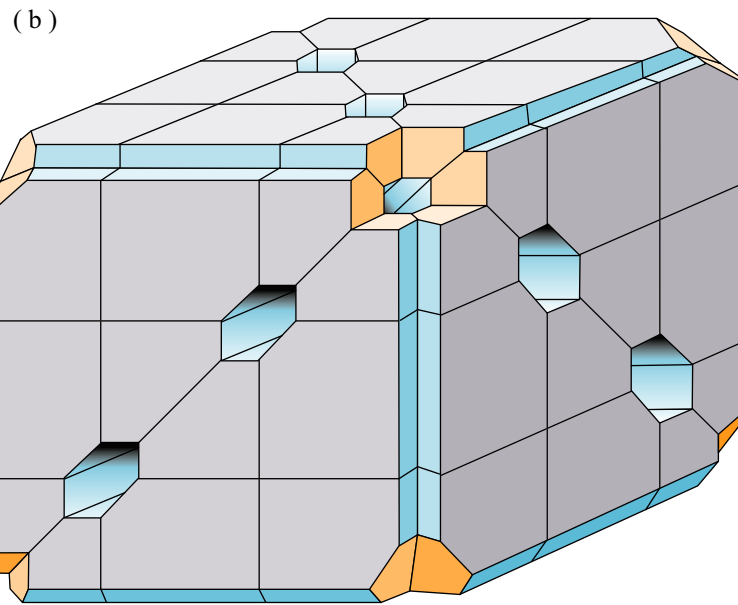
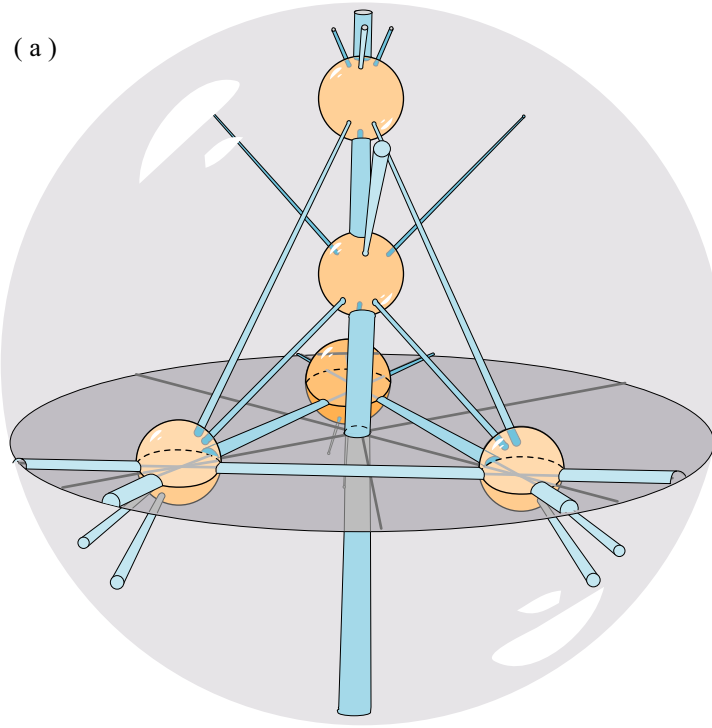


FIGURE 13. Iterated blow-ups of (a) $\mathbb{R}P^3$ to $PV_{\#}^3$ and (b) T^3 to $\overline{\mathcal{M}}_0^6(\mathbb{R})$ are both homeomorphic with a tiling by 60 associahedra.